for a thermal state. Far above threshold, the pulse width only decreases further and therefore $g^{(2)}(0)$ remains a good estimate for $g^{(2)}(0)$. However the $g^{(2)}(0)$ measured in this region decreases, demonstrating that second-order coherence, or in other words, a quantum-mechanical pure state, is forming in the polariton condensate.

In conclusion, the quantum phase transition from a classical thermal mixed state to a quantum-mechanical pure state in an exciton polariton system is confirmed by observing the decrease of $g^{(2)}(0)$ above threshold. It is still an open question what specific quantum state the condensate falls into. A standard BEC theory suggests a particle number eigenstate at absolute zero temperature. The quantum Monte-Carlo wavefunction analysis based on the exciton-phonon coupling in an open system suggests a coherent state (*25*). However, the interactions among polaritons leads to virtual excitations of quantum correlated pair excited states (*26*, *27*), which resembles a squeezed state in quantum optics. For all of these cases, $g^{(2)}(0)$ is expected to approach one, so the present experiment does not distinguish among these possible quantum states. Fortunately, due to the half matter–half light nature of the polaritons (*28*), their coherence properties are transferred to the emitted light field. They then can be measured with methods well developed in quantum optics such as higher-order coherence functions and optical homodyne tomography (*29*). Future research along this line should clarify the exact nature of the quantum state that the polariton condensate approaches above threshold.

References and Notes

1. R. J. Glauber, *Phys. Rev.* **130**, 2529 (1963).
2. W. Ketterle, H. J. Miesner, *Phys. Rev. A* **56**, 3291 (1997).
3. E. A. Burt *et al.* , *Phys. Rev. Lett.* **79**, 337 (1997).
4. A. Griffin, D. W. Snoke, S. Stringari, *Bose-Einstein Condensation* (Cambridge Univ. Press, Cambridge, 1995).
5. S. A. Moskalenko, D. W. Snoke, *Bose-Einstein Condensation of Excitons and Biexcitons and Coherent Nonlinear Optics with Excitons* (Cambridge Univ. Press, New York, 2000).
6. C. Weisbuch, M. Nishioka, A. Ishikawa, Y. Arakawa, *Phys. Rev. Lett.* **69**, 3314 (1992).
7. M. Kuwata-Gonokami *et al.*, *Phys. Rev. Lett.* **79**, 1341 (1997).
8. F. Tassone, Y. Yamamoto, *Phys. Rev. B* **59**, 10830 (1999).
9. L. S. Dang, D. Heger, R. André, F. Boeuf, R. Romestain, *Phys. Rev. Lett.* **81**, 3920 (1998).
10. P. Senellart, J. Bloch, *Phys. Rev. Lett.* **82**, 1233 (1998).
11. G. Dasbach, T. Baars, M. Bayer, A. Larionov, A. Forchel, *Phys. Rev. B* **62**, 13076 (2000).
12. R. Huang, F. Tassone, Y. Yamamoto, *Phys. Rev. B* **61**, R7854 (2000).
13. R. Huang *et al.*, *Phys. Rev. B* **65**, 165314 (2002).
14. J. Bloch, T. Freixanet, J. Marzin, V. Thierry-Mieg, R. Planel, *Appl. Phys. Lett.* **73**, 1694 (1998).
15. M. Saba *et al.*, *Nature* **414**, 731 (2001).
16. J. B. Khurgin, *Solid State Commun.* **117**, 307 (2000).
17. J. J. Baumberg *et al.*, *Phys. Rev. B* **62**, R16247 (2000).
18. C. Ciuti, P. Schwendimann, A. Quattropani, *Phys. Rev. B* **63**, R041303 (2001).
19. n_{QW} is estimated from the number of pump photons per pulse ($\sim 5 \times 10^7$) multiplied by the absorption per quantum well ($\sim$1%) and the percentage of the pump light coupled into the microcavity ($\sim$5%). For a spot of $D \approx 20$ μm in diameter, $n_{QW} \approx 8 \times 10^9$ cm^{-2} per pulse. n_{LP} at threshold is estimated to be $\sim$1 by $N_{LP} = n_{LP} M \eta f_P \Delta T_p / \tau_{LP}$ with the following parameters: the detected photon flux $N_{LP} = 2500$ s^{-1}, the repetition rate of the mode-locked pump laser $f_P = 76$ MHz , the overall detection efficiency $\eta \sim 10^{-4}$, the emitted pulse duration $\Delta T_p \sim 10$ ps, LP lifetime $\tau_{LP} \sim 3$ ps, and $M =$ $\frac{1}{2}\frac{\pi D^2/4}{4\pi^2}\frac{\pi(k_0\Delta\theta)^2}{4}$ is the number of transverse states subtended by the acceptance angle of the detector $\Delta\theta \sim 0.01$. $k_0 = 8.15 \times 10^4$ cm^{-1} is the freespace logitudinal wavenumber of the cavity photon.
20. C. Ciuti, P. Schwendimann, B. Deveaud, A. Quattropani, *Phys. Rev. B* **62**, R4825 (2000).
21. H. Cao *et al.*, *Phys. Rev. A* **55**, 4632 (1997).
22. M. Kira *et al.*, *Phys. Rev. Lett.* **79**, 5170 (1997).
23. P. G. Savvidis *et al.*, *Phys. Rev. Lett.* **84**, 1547 (2000).
24. C. W. Gardiner, P. Zoller, *Quantum Noise* (Springer-Verlag, New York, 2000).
25. A. Imamoglu, R. Ram, *Phys. Lett. A* **214**, 193 (1996).
26. M. Naraschewski, R. J. Glauber, *Phys. Rev. A* **59**, 4595 (1999).
27. F. Tassone, Y. Yamamoto, *Phys. Rev. A* **62**, 063809 (2000).
28. Y. Yamamoto, *Nature* **405**, 629 (2000).
29. D. Smithey, M. Beck, M. Raymer, A. Faridani, *Phys. Rev. Lett.* **70**, 1244 (1993).

29 May 2002; accepted 29 August 2002

Dynamics of Hydrogen Bromide Dissolution in the Ground and Excited States

S. M. Hurley, T. E. Dermota, D. P. Hydutsky, A. W. Castleman Jr.*

The dissolution of acids is one of the most fundamental solvation processes, and an important issue is the nature of the hydration complex resulting in ion pair formation. We used femtosecond pump-probe spectroscopy to show that five water molecules are necessary for complete dissolution of a hydrogen bromide molecule to form the contact ion pair $H^+{\cdot}Br^-(H_2O)_n$ in the electronic ground state. In smaller mixed clusters ($n < 5$), the ion pair formation can be photoinduced by electronic excitation.

In many areas of atmospheric and biological chemistry, the dissolution of acids in aqueous media is of fundamental importance. One of the basic processes of interest is the acid ionization of hydrogen bromide (HBr) molecules in aqueous media to form the contact ion pair $H^+{\cdot}Br^-$, which has been the subject of many theoretical studies (*1*–*5*) but relatively few experimental studies (*6*). One extensively discussed issue is the minimum number of water molecules that is necessary to solvate the molecule and form the contact ion pair in isolated complexes. Theoretical calculations (*1*–*3*) predict that contact ion pair formation starts to occur in the mixed cluster containing three water molecules, and by the $n = 4$ mixed cluster, complete dissolution has occurred. Here, we report an investigation into the ultrafast dynamics of mixed clusters of HBr-water, using the pump-probe technique (*7*) coupled with reflectron time-of-flight mass spectrometry (*8*, *9*) to determine the mechanism of ion pair formation in the ground and excited electronic states of HBr.

A molecular beam composed of HBr clusters was formed by the supersonic expansion through a pulsed nozzle (150 μm in diameter) of a 10% HBr (Matheson gas) mixture seeded in argon maintained at a total backing pressure of ~3 bar. Mixed HBr-water clusters were formed by crossing the neutral cluster beam with an effusive water vapor beam from a pickup source (*10*). A (2 + 1) pump-probe ionization scheme (pump, 271 nm; probe, 407 nm; pulse duration, 80 fs) was used to study the dynamics of HBr-water clusters excited to the $v = 1$ level of the Rydberg $C^1\Pi$ state of the HBr chromophore (*11*). Mass spectra revealed a typical cluster distribution, including HBr clusters up to size 10, $H^+(H_2O)_n$ ($n = 1$ to 4) and mixed clusters of $H^+(HBr)(H_2O)_n$ ($n = 1$ to 3). In Fig. 1A, the pump-probe temporal responses of HBr^+ and H_2O^+ are shown. The transient pump-probe dynamics of the protonated water clusters (Fig. 1B) are substantially different from those of the HBr^+ and H_2O^+ monomers (Fig. 1A). The $H^+(H_2O)_n$ originate from a mixed cluster of HBr and water. The excess proton in the product originates from the HBr, as established through extensive studies of the isotopically substituted acids. After ionization of the mixed cluster, a neutral bromine is lost, and only protonated water clusters are detected, as depicted in Eq. 1.

$$HBr(H_2O)_n + (2+1)h\nu \rightarrow H(H_2O)_n{}^+ + Br + e^- \qquad (1)$$

where h is Planck's constant and ν is frequency. Under the conditions of the present experiments, water is added effusively, and neutral water clusters are not formed; hence,

---

Departments of Chemistry and Physics, Pennsylvania State University, University Park, PA 16802, USA.

*To whom correspondence should be addressed. E-mail: awc@psu.edu

the only source of the detected species is a mixed cluster $HBr(H_2O)_n$, formed by replacement reactions of water with HBr clusters. This conclusion was verified by experiments conducted in the absence of HBr. Other experiments were conducted with $DBr(H_2O)_n$ that resulted in $D^+(H_2O)_n$ as the product through a reaction analogous to Eq. 1. This confirmed that the excess proton in the water clusters originated from the acid. We also obtained results for clusters containing multiples of HBr (*12*).

Anticipating results from pump-probe spectroscopic experiments, we considered three possible situations: (i) for very small clusters, the pump-probe temporal response would be similar to that of the acid, mediated by the dynamics of energy transfer and/or molecular rearrangement upon photoexcitation; (ii) the absorption of a photon would result in a photoinduced rearrangement and ion pair formation; and (iii) in sufficiently large cluster sizes, ion pair formation would occur in the ground state, making the absorption coefficient required in the initial pump processes distinctly different from that of the molecular HBr complex.

One of the aims of this study was to experimentally determine the minimum number of water molecules (*n* in Eq. 1) necessary to solvate an HBr molecule to form the contact ion pair $H^+{\cdot}Br^-(H_2O)_n$ for comparison with theoretical predictions. The dynamics observed in these studies show that photochemistry coupled with solvation and clustering of HBr with water molecules involve complex rearrangement and reaction pathways resulting in the formation of the ion pair. Solvation has a strong influence on the dynamics of the observed clusters, and a simple exponential decay of the excited species was not observed for any of the protonated water clusters. The transient behavior was fit to a sum of a Gaussian response near the temporal overlap (zero delay time) of the pump and probe beams and an exponential rise at later delay times (*12*).

Theoretical (*13*), spectroscopic (*14*, *15*), and dynamic (*16*) studies have shown that some of the Rydberg states of HBr can interact with the valence ion pair states. The energy shift upon the solvation of the valence ion pair state is expected to be larger than that for the Rydberg states because of the charge-dipole interaction (*17*). Thus, the energy of the valence states is lowered much more than that of the Rydberg states. In mixed clusters of HBr-water, where acid ionization has not occurred in the ground state, the ion pair can be photoinduced to form by the following mechanism. An $HBr(H_2O)_n$ cluster is formed in the molecular beam, and a two-photon absorption promotes the complexed HBr molecule to the $C^1\Pi$ state, shifted in energy by the interaction with the water molecules. Electronic and vibrational excitation of the HBr molecule by the pump photons results in the formation of the ion pair. Solvation, as depicted in Fig. 2, lowers the energy of the $V^1\Sigma^+$ state so that it is accessible from the $C^1\Pi$ state by internal conversion. In the unsolvated case, the valence state is not energetically accessible. Because of the small absorption cross section of the $V^1\Sigma^+$ valence state (*11*), the ionization probability is low. The data in Fig. 1 reveal that as the ion pair forms, the solvent reorganizes about the ion core. In simulations of the acid ionization of HCl in water clusters, Ando and Hynes have shown that solvent reorganization follows the formation of the contact ion pair (*18*). As the solvent reorganizes around the $H^+{\cdot}Br^-$ ion core, the absorption cross section increases, resulting in an increase in the ion signal and thus a rise in the pump-probe traces.

The ionization potentials (IPs) of HBr and $HBr(H_2O)$ were calculated with the program GAMESS (*19*), with a 6-31G basis set having additional diffuse and polarizable functions added. Geometries were optimized with the unrestricted Hartree-Fock computational method, followed by energy calculations with the MP2 level of theory. Although not a high-level calculation, it is sufficient to account for the energy differences responsible for our findings. For a vertical process, the vertical IP of HBr is 11.7 eV, whereas that of $HBr(H_2O)$ is calculated to be ~11.0 eV, showing that solvation lowers the IP by 0.7 eV (Fig. 3). In the adiabatic ionization process, $HBr(H_2O)$ is rearranged to yield the proton-transferred dimer ion

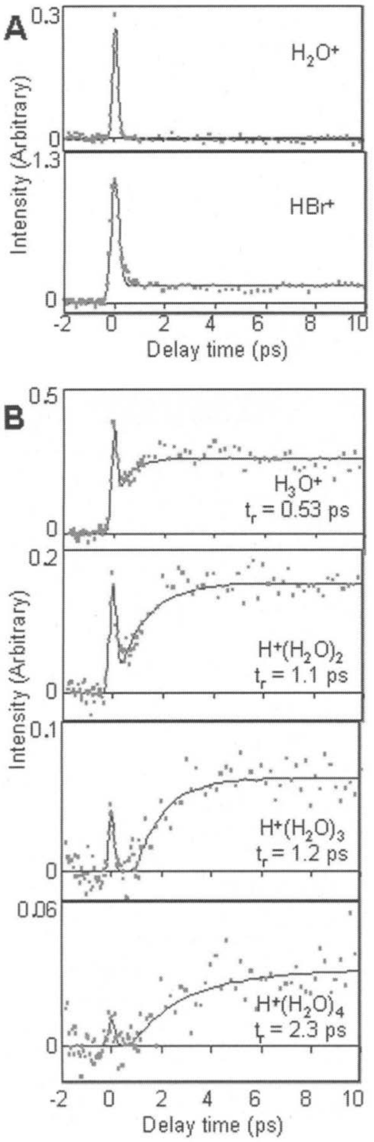

Fig. 1. Pump-probe temporal response with a pump wavelength of 271 nm of (**A**) monomers of water showing a pulse width–limited decay and HBr showing a long lifetime and (**B**) protonated water clusters exhibiting dynamics unlike those of the monomers. The best fit of the data (squares) is shown by the solid line, where t_r is the rise time.

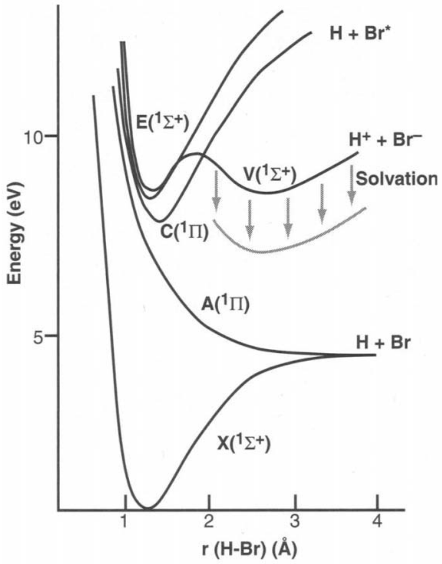

Fig. 2. Potential energy surface of HBr. Downward arrows qualitatively indicate solvation of the $V(^1\Sigma^+)$ valence state [adapted from (*15*)]. *r*, internuclear separation.

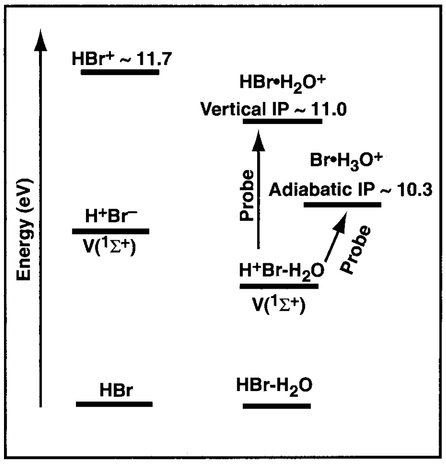

Fig. 3. Ionization potentials for HBr and $HBr(H_2O)$, calculated with GAMESS. The left side of the figure shows the energy levels for the unsolvated HBr molecules. The right side of the figure shows the shift in the energy levels due to solvation and solvent reorganization.

$(\mathrm{Br{\cdot}H_3O})^+$. The calculated IP of this species is ~10.3 eV, which is lower than the IP of the molecular complex by 0.7 eV. Such a dramatic change in the energetics with solvent rearrangement implies that the ability to detach the electron from the fully solvated complex (solvent-separated ion pair) should increase.

In agreement with this expectation, the data in Fig. 1 show that as the degree of solvation increases, so does the rise time of the pump-probe response. Because the rise in the pump-probe response is sensitive to the solvent reorganization about the contact ion pair, the amount of time it will take for the molecules to reorganize to form the solvent-separated ion pair will increase with the number of solvent molecules surrounding the ion pair core. Similar results were observed for protonated HBr clusters, which indicate that self-solvation can induce ion pair formation in the excited state by a mechanism analogous to solvation by water molecules (*12*).

According to theoretical predictions (*1–3*), ion pair formation should begin in mixed clusters $[\mathrm{HBr(H_2O)}_n$ with $n = 3]$; and in clusters with $n = 4$ or higher, complete dissolution should occur. If the ion pair forms in these species as suggested, upon sufficient hydration it should become observable in the ground state without being photon-mediated. Formation of the ion pair should also alter the potential energy surface so that photon absorption should not occur in the same way as it does in the case of the hydrated complex, in which the molecular nature of HBr is retained. The ion intensity at the zero delay time decreases with increasing cluster size. This decrease in intensity is attributed to the formation of the ion pair in the ground state. An increase in the H-Br internuclear separation accompanies the formation of the ion pair and is expected to result in a decrease in the absorption cross sections for photons of the same frequency. The observed rise in the signal of the $\mathrm{H^+(H_2O)_4}$ cluster shows that a substantial population rearranges on the picosecond time scale to form the fully solvated ion pair $\mathrm{H^+(H_2O)_4{\cdot}Br^-}$ in the excited state. Thus, complete ion pair formation could not have occurred in the ground state at $n = 4$, and a portion of the species in the molecular beam exists in the molecular $\mathrm{HBr(H_2O)_4}$ form rather than the ion pair form.

In the mass spectra, we observed $\mathrm{H^+(H_2O)}_n$ with $n = 1$ to 4, whereas HBr clusters were readily observed with sizes ranging up to 10. We found that water replacement in the acid clusters was facile at all cluster sizes; therefore, failure to observe the $n = 5$ cluster was not due to intensity issues. From the large change in the cross section at $n = 4$, and particularly from the lack of observation of an $n = 5$ protonated water cluster (despite observing the larger clustered HBr species), we conclude that this represents evidence that the cluster size for complete dissolution is five water molecules. In clusters smaller than this, ion pair formation can be induced by electronic excitation. The theoretical predictions (*1–3*) of HBr dissolution were determined for equilibrium structures, whereas the experiments were performed at a finite temperature, though accurate knowledge of the molecular beam temperature was not known. Therefore, our experimental findings of complete dissolution of HBr by water at the $n = 5$ cluster size can be considered to be in reasonably good agreement with the theoretical predictions.

References and Notes

1. B. J. Gertner, G. H. Peslherbe, J. T. Hynes, *Isr. J. Chem.* **39**, 273 (1999).
2. C. Conley, F. M. Tao, *Chem. Phys. Lett.* **301**, 29 (1999).
3. M. Tachikawa, *Mol. Phys.* **100**, 881 (2002).
4. S. H. Robertson, D. C. Clary, *Faraday Discuss.* **100**, 309 (1995).
5. A. Al-Halabi, R. Bianco, J. T. Hynes, *J. Phys. Chem. A* **106**, 7639 (2002).
6. J. Gilligan, A. W. Castleman Jr., *J. Phys. Chem. A* **105**, 5601 (2001).
7. T. S. Rose, M. J. Rosker, A. H. Zewail, *J. Chem. Phys.* **91**, 7415 (1989).
8. J. Breen, K. Kilgore, W. B. Tzeng, S. Wei, A. W. Castleman Jr., *Chem. Phys.* **90**, 11 (1989).
9. Q. Zhong, L. Poth, J. V. Ford, A. W. Castleman Jr., *J. Phys. Chem. B* **101**, 4203 (1997).
10. L. Poth, Z. Shi, Q. Zhong, A. W. Castleman Jr., *Int. J. Mass Spectrom. Ion Processes* **154**, 35 (1996).
11. J. B. Nee, M. Suto, L. C. Lee, *J. Chem. Phys.* **85**, 4919 (1986).
12. S. M. Hurley, T. E. Dermota, D. P. Hydutsky, A. W. Castleman Jr., in preparation.
13. D. A. Chapman, K. Balasubramanian, S. H. Lin, *Chem. Phys.* **118**, 333 (1987).
14. A. Kvaran, A. Logadottir, H. Wang, *J. Chem. Phys.* **108**, 5856 (1998).
15. A. Kvaran, H. Wang, A. Logadottir, *J. Chem. Phys.* **112**, 10811 (2000).
16. S. M. Hurley, Q. Zhong, A. W. Castleman Jr., *J. Chem. Phys.* **112**, 4644 (2000).
17. C. Dedonder-Lardeux, G. Grégoire, C. Jouvet, S. Martrenchard, D. Solgadi, *Chem. Rev.* **100**, 4023 (2000).
18. K. Ando, H. T. Hynes, *J. Phys. Chem. B* **101**, 10464 (1997).
19. M. W. Schmidt *et al.*, *J. Comput. Chem.* **14**, 1347 (1993).

20. Financial support by the Atmospheric Sciences Division and the Experimental Physical Chemistry Division of NSF, grant NSF-089233, is gratefully acknowledged. Computational support was provided by the Materials Simulation Center, a facility of the Materials Research Institute at the Pennsylvania State University.

20 June 2002; accepted 28 August 2002

Selective and Efficient Platinum(0)-Carbene Complexes As Hydrosilylation Catalysts

István E. Markó,[1]* Sébastien Stérin,[3] Olivier Buisine,[3] Gérard Mignani,[3] Paul Branlard,[3] Bernard Tinant,[2] Jean-Paul Declercq[2]

The hydrosilylation reaction enables the production of silicon polymers. Platinum-carbene complexes are reported that catalyze the hydrosilylation reaction of alkenes with remarkable efficiency and exquisite selectivity and avoid the formation of platinum colloids. By-products, typically encountered with previous catalytic systems, are suppressed with these platinum derivatives.

The hydrosilylation reaction, the addition of a Si-H unit to a C-C double bond to form an alkylsilane (Fig. 1A) (*1–3*), enables the production of silicon polymers used in silicon rubbers, liquid injection molding products, paper release coatings, and pressure-sensitive adhesives (*4*). The hydrosilylation reaction can be initiated or catalyzed in numerous ways (*5*). Among these, the use of metal salts, supported metals, and transition metal complexes are the most common, with platinum derivatives being overwhelmingly preferred (*6*). Two Pt-based systems, the Speier (*7*) catalyst ($\mathrm{H_2PtCl_6/{}^iPrOH}$) and the Karstedt catalyst **8** (Fig. 1C), have found widespread use in the silicone industry (*8*).

Unfortunately, hydrosilylation by Karstedt catalyst **8** suffers from a number of drawbacks, including the formation of significant amounts (20 to 40%) of the isomeric olefins **4** and **5**, the reduced alkene **6**, and the dehydrocondensation adduct **7** (Fig. 1A) (*9*). If these impurities are not removed in a subsequent postreaction treatment, they lead to deleterious effects on the quality or properties of the final materials. In addition, the formation of colloidal Pt species during the course of the hydrosilylation reaction often results in undesired side reactions and coloration of the final product (*10*, *11*). We now report that readily available platinum(0)-carbene complexes catalyze the hydrosilylation reaction with remarkable efficiency and exquisite selectivity and, in many cases, produce almost exclusively adduct **3** (*12*).

---

[1]Unité de Chimie Organique et Médicinale and [2]Unité d'Analyse Structurale, Département de Chimie, Université Catholique de Louvain, Place Louis Pasteur 1, 1348 Louvain-la-Neuve, Belgium. [3]Rhodia Silicones, Avenue des Frères Perret 55, F69192 Saint-Fons Cedex, France.

*To whom correspondence should be addressed. E-mail: marko@chim.ucl.ac.be